Magnetic phase diagram of (Cr$_{1-x}$Mo$_x$)$_{0.986}$Si$_{0.014}$

Magnetic phase diagram of $(Cr_{1-x} \, Mo_x)_{0.986} Si_{0.014}$

P Smit and H L Alberts

Physics Department, Rand Afrikaans University, PO Box 524, Johannesburg 2000, South Africa

Abstract. The magnetic phase diagram of $(Cr_{1-x}Mo_x)_{0.986}Si_{0.014}$ for $0 < x \leq$ 12%, as determined from electrical resistivity, ultrasonic wave velocity and thermal expansion measurements, has both commensurate and incommensurate spin-density-wave regions. The results are discussed in terms of the two-band imperfect nesting model, taking changes in the nesting parameter into account. The phase diagram is fairly well explained by assuming changes in the nesting parameter on alloying to be the dominant effect. Effects of d-band broadening, impurity scattering and changes of density of states on alloying seem to play a relatively lesser role in changing the Néel point and the magnetic phases on alloying. Mo appears to act as an electron acceptor in the alloys.

1. Introduction

The incommensurate (I) spin density wave (SDW) antiferromagnetic state of pure Cr is a consequence of nesting of the electron and hole sheets of its Fermi surface (Lomer 1964). In their theory of the SDW state of Cr, Machida and Fujita (1984) (see also Fujita and Machida 1987) used an energy misfit or nesting parameter, $H = \frac{1}{2}\hbar v_F(k_e - k_h)$, to describe the difference in sizes of the two Fermi surface sheets. The sizes of the electron and hole Fermi surfaces are characterized by k_e and k_h respectively, and v_F is the Fermi velocity. On alloying Cr with other elements to form Cr-rich alloys, the SDW state is mainly influenced through three mechanisms. Firstly, changes in the electron-to-atom (e/a) ratio on alloying induce changes in H which influence the SDW state. Machida and Fujita (1984) showed theoretically that increasing H from its value of pure Cr, on alloying for instance with V to decrease the e/a ratio, results in a decrease in the Néel temperature (T_N), while the system remains in the ISDW state at all temperatures below T_N. On the other hand, it is shown that a decrease in H, corresponding to an increase in e/a (on alloying for instance with Mn), results in an appearance of a commensurate (C) SDW state and an increase in T_N. The positions of the ISDW-paramagnetic (P), CSDW–P and ISDW–CSDW transition lines of the magnetic phase diagram caused by changes in H were calculated by Machida and Fujita (1984) using a two band imperfect-nesting model.

Secondly, d-band broadening may result on alloying which, as discussed by Koehler *et al* (1966), suppresses SDW formation leading to a 'weakened' SDW state and a decrease in the Néel temperature. This mechanism plays an important role in the case of Cr–Mo alloys (Cywinski and Hicks 1986) where Mo, which is isoelectronic with Cr, lowers the T_N of Cr to 0 K on alloying with more than 24 at.% Mo.

The third mechanism results from a pair-breaking mechanism (Behera and Viswanathan 1969, Dadârlat *et al* 1980) caused by impurity scattering. This effect always lowers T_N by destabilising the SDW state. Dadârlat *et al* (1980) consider both scattering effects and changes in the density of states resulting from distortions of the Fermi surface on alloying to calculate T_N for Cr–Si alloys. Effects of changes in the density of states on T_N are not included in the theory of Machida and Fujita (1984).

In the 'Si-series' ternary alloy system, $(Cr_{0.97}Mo_{0.03})_{1-x}Si_x$, (Smit and Alberts 1989) it was found that the CSDW transition phase of the Cr–Si system (Alberts and Lourens 1988), is completely suppressed on adding Si to $Cr_{0.97}Mo_{0.03}$, i.e. to a magnetically weakened Cr. The results for this series could be well explained assuming that the third mechanism plays the dominant role. Effects of changes in H seem to be small compared to the effects of impurity scattering and changes in the density of states on alloying. Mo in $(Cr_{0.97}Mo_{0.03})_{1-x}Si_x$ weakens the SDW state of pure Cr through d-band broadening.

In this paper we report the magnetic phase diagram of another series in the Cr–Mo–Si ternary system, namely the 'Mo series' $(Cr_{1-x}Mo_x)_{0.986}Si_{0.014}$. In contrast to the Si series, it is found that changes in H (the first mechanism) play an important role in altering T_N and the magnetic phases of the Mo series. Furthermore, although Mo acts in binary Cr–Mo alloys to a first approximation not to alter e/a (Cywinski and Hicks 1986), it plays the role of an electron acceptor in the Mo series.

2. Experimental procedure and results

Polycrystalline $(Cr_{1-x}Mo_x)_{0.986}Si_{0.014}$ alloy ingots with $x = 0.0006, 0.0013, 0.0025, 0.0038, 0.005, 0.01, 0.03, 0.05, 0.065, 0.1$ and 0.12 were prepared from 99.99% Cr and Mo and 99.999% Si starting materials by argon arc-melting, as described by Smit and Alberts (1986). The alloys were homogenised at 1000 °C for 72 h. X-ray diffraction methods revealed only BCC lines. Electron microprobe analyses showed the samples to be of good homogeneity and concentrations determined by means of atomic absorbtion and induction-coupled plasma (ICP) atomic emission techniques compare well with the nominal concentrations quoted above.

Measurements of electrical resistivity, thermal expansion and ultrasonic longitudinal wave velocities as function of temperature were made to determine the magnetic properties of the alloys (Smit and Alberts 1987, Alberts and Lourens 1983, 1984). Data sampling in the temperature range 4–450 K took place at 0.5 K intervals, but in the case of ultrasonic wave velocities, it took place at 1–2 K intervals. The experimental error in the absolute value of electrical resistivity, ρ, amounts to about 1%, and 2% for ultrasonic longitudinal wave velocities, v_L, whereas in the case of $\Delta L/L$ and the thermal expansion coefficient, α, the absolute errors are estimated to be of the order of 5 and 10%, respectively. Furthermore, changes in the order of one in 10^4 with temperature were easily detected.

The thermal expansion measurements of the Cr–Mo–Si system were conducted relative to those of paramagnetic Cr + 5 at.% V to obtain the contributions of the magnetic ordering in the Cr–Mo–Si alloys (Alberts and Lourens 1984). This procedure enables us to measure the temperature dependence of

$$\left(\frac{\Delta L}{L}\right)_{Cr_{0.95}V_{0.05}} - \left(\frac{\Delta L}{L}\right)_{CrMoSi} = \left(\frac{\Delta L}{L}\right)_{para\,CrMoSi} - \left(\frac{\Delta L}{L}\right)_{CrMoSi}$$

directly, assuming that the paramagnetic behaviour of Cr–Mo–Si closely resembles that of $Cr_{0.95}V_{0.05}$ down to 0 K as was done previously for other Cr alloys (Alberts and Lourens 1988, Van Rijn *et al* 1987, Venter *et al* 1986). Differentiation of the $\Delta L/L$ versus T curves with respect to T, yields the temperature dependence of the magnetic contribution to the coefficient of thermal expansion, namely

$$\Delta \alpha = \alpha_{\text{para CrMoSi}} - \alpha_{\text{CrMoSi}} \tag{1}$$

The results of Roberts *et al* (1983) for $Cr_{0.95}V_{0.05}$ were used in conjunction with equation (1) to determine α_{CrMoSi} for each alloy. Figure 1 represents a typical example of the temperature dependence of α.
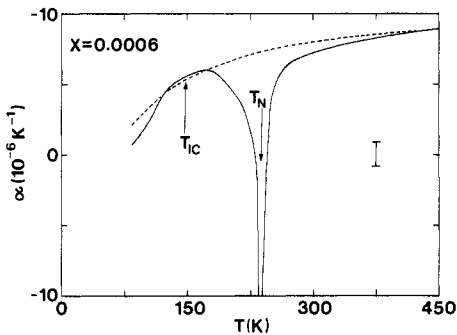
Figure 1. The variation of the coefficient of thermal expansion, α, with temperature for $(Cr_{1-x}Mo_x)_{0.986}Si_{0.014}$ with $x = 0.0006$. The broken line represents α for $Cr_{0.95}V_{0.05}$ (Roberts *et al* 1983) which resembles the paramagnetic state of the Cr–Mo–Si system.
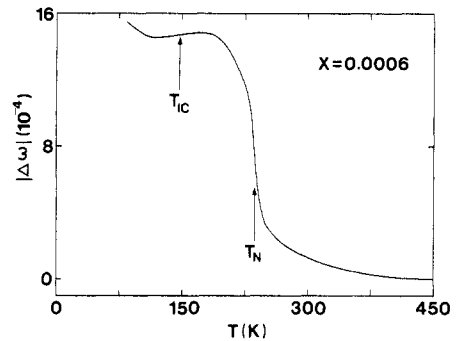
Figure 2. Temperature dependence of the absolute value of the magnetovolume for $(Cr_{1-x}Mo_x)_{0.986}Si_{0.014}$ with $x = 0.0006$, determined from figure 1 via integration.

Numerical integration of the α versus T curves gives the magnetovolume

$$\Delta\omega(T) = 3 \int_0^T \Delta\alpha \, dT - 3 \int_0^{T_f} \Delta\alpha \, dT$$

where T_f denotes the maximum temperature over the range measurements were conducted. Figure 2 depicts the magnetovolume ($\Delta\omega$) determined from the α versus T curve of figure 1.

The magnetic transition temperatures of the $(Cr_{1-x}Mo_x)_{0.986}Si_{0.014}$ alloys for $0 < x \leq 0.065$ were determined from the observed magnetic anomalies in the (ρ, T), (v_L, T) and $(\Delta\omega, T)$ curves as was done for other Cr alloys (Alberts and Lourens 1988). Typical examples of the behaviour of ρ, v_L and $\Delta L/L$ are shown in figure 3. For samples with $x = 0.0006$ and 0.0013, very large ultrasonic attenuation was observed near the Néel temperature, to such an extent that the ultrasonic echos were undetectable in a certain temperature range near T_N making measurements of v_L in this temperature range impossible. This is reflected in the results of figure 3(c) which shows a typical example. This behaviour seems to be typical of a first order CSDW–P transition in Cr alloys and was previously reported also in Cr–Si alloys by Alberts and Lourens (1988) and also found in Cr–Fe alloys by Alberts (private communication). We therefore take
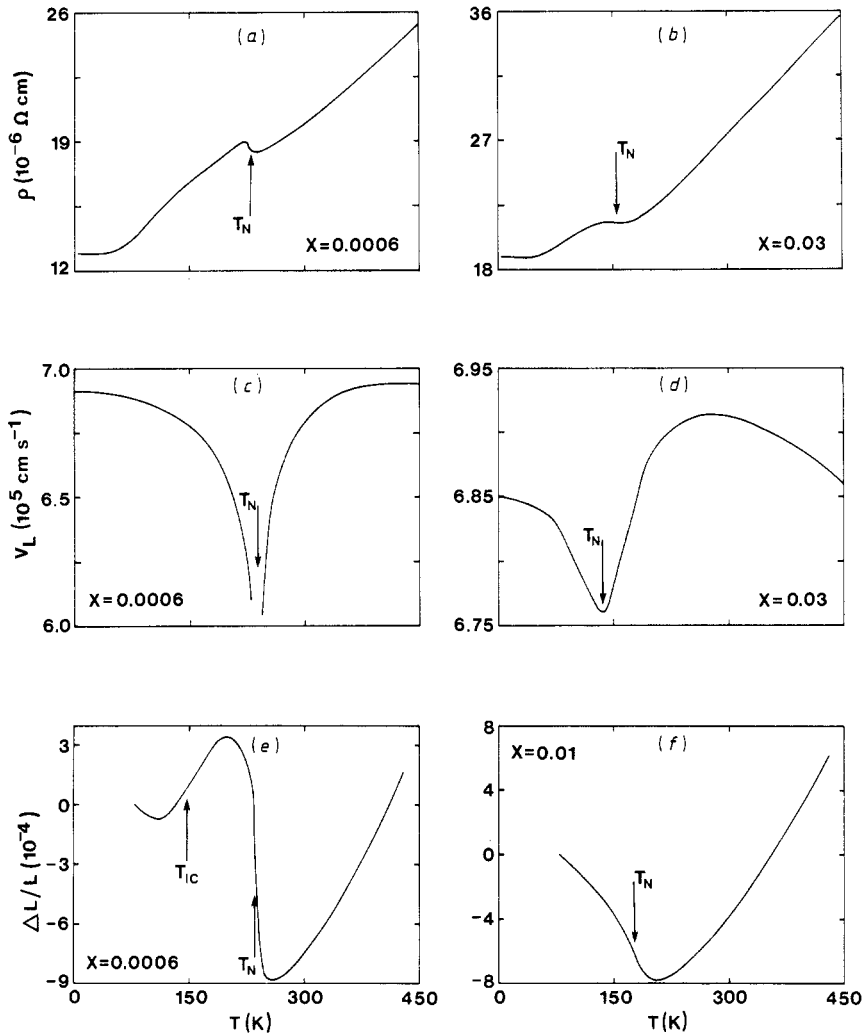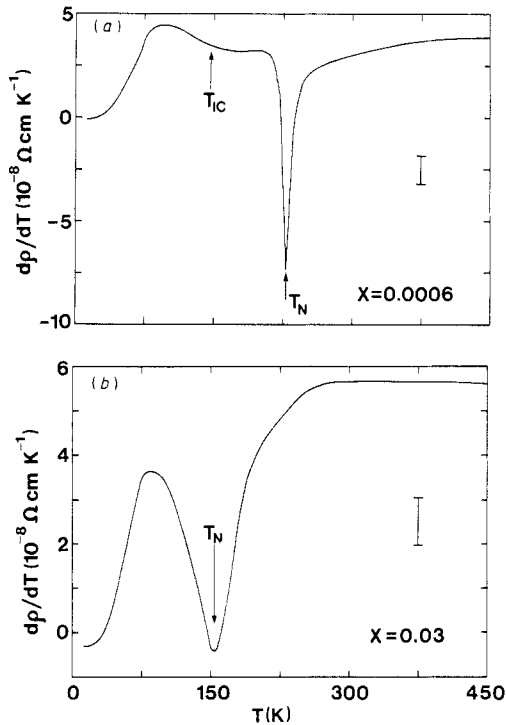
Figure 3. Typical temperature dependence for $(Cr_{1-x}Mo_x)_{0.986}Si_{0.014}$ of ρ with (a) $x = 0.0006$ and (b) $x = 0.03$, v_L with (c) $x = 0.0006$ and (d) $x = 0.03$ and $\Delta L/L$ with (e) $x = 0.0006$ and (f) $x = 0.01$. Samples with $x = 0.0006$ ((a), (c) and (e)) depict first-order transitions at T_N, as indicated by the arrows while for $x = 0.01$ and 0.03 ((b), (d) and (f)) the transitions are of second-order. The T_{IC} in (e) depicts the I–C transition with a value determined from $d(\Delta\omega)/dT$. The curves shown are smoothed through the experimental points, with sampling taking place at 0.5 K intervals for ρ and $\Delta L/L$, while in the case of v_L, the sampling took place at 1–2 K intervals.

the transition at T_N for alloys with $x = 0.0006$ and 0.0013 to be first order CSDW–P transitions. The first order transition for these alloys was also exhibited to a lesser extent in the behaviour of ρ versus T and of $\Delta L/L$ versus T. These two quantities show almost jump-like behaviour at T_N similar to that observed in the Cr–Si system (Alberts and Lourens 1988) at the first order CSDW–P transition (figures 3(a) and 3(e)). In the case of alloys with $x = 0.0025$, 0.0038 and 0.005 the results were not conclusive enough to determine whether the transition at T_N was first order or not.

The large ultrasonic attenuation and near step-like behaviour at T_N were definitely

absent from alloys with $0.01 \leq x \leq 0.065$ (figures 3(b), 3(d) and 3(f)) suggesting, as was also found for the Cr–Si system by Alberts and Lourens (1988), a second order ISDW–P transition at T_N for these alloys. For $x > 0.065$ no anomalies were observed in the temperature behaviour of ρ, v_L or $\Delta L/L$, suggesting that they remain paramagnetic throughout the temperature range 4–450 K. The transition temperature T_N was defined as the temperature at the minimum of the curve, in the case of ultrasonic longitudinal wave velocity measurements, and for the ρ and $\Delta\omega$ versus T curves as the temperature where $d\rho/dT$ (Smit and Alberts 1987) and $d(\Delta\omega)/dT$ are minima.

Figure 4. Temperature dependence of $d\rho/dT$ for $(Cr_{1-x}Mo_x)_{0.986}Si_{0.014}$ with (a) $x = 0.0006$ and (b) $x = 0.03$, determined through differentiation of the curves from figures 3(a) and (b). The flat region, $T < T_N$, as displayed in (a) for $x = 0.0006$, resembles an I–C transition where the value of T_{IC} was determined from $d(\Delta\omega)/dT$.

Usually ISDW–CSDW phase transitions are clearly seen in thermal expansion measurements of Cr alloys which exhibit a second anomaly at the transition temperature $T_{IC} < T_N$. This was observed as peaks in α-T curves near T_{IC} of Cr–Si alloys by Alberts and Lourens (1988). In the case of the $(Cr_{1-x}Mo_x)_{0.986}Si_{0.014}$ ternary alloys similar effects were observed for $0 < x \leq 0.005$ indicating I–C transitions in them. The presence of the ISDW and CSDW phases in the ternary Cr–Mo–Si alloys was inferred from the known behaviour of binary Cr–Si alloys (Endoh *et al* 1982, Alberts and Lourens 1988). An example of the I–C transition in Cr–Mo–Si is shown in figure 1. For these alloys T_{IC} is defined (Alberts and Lourens 1988) at the temperature of the lower temperature inflection point on the $\Delta\omega$–T curves as in figure 2. The transition at T_{IC} in these alloys is furthermore accompanied by broad flat regions in the $d\rho/dT$–T curves (figure 4(a)) similar to those observed in the Si series (Smit and Alberts 1989). These regions are absent in those alloys not exhibiting I–C transitions

as shown in the example of figure 4(b). No anomaly is observed at T_{IC} in the $v_L - T$ curves of the $(Cr_{1-x}Mo_x)_{0.986}Si_{0.014}$ alloys.
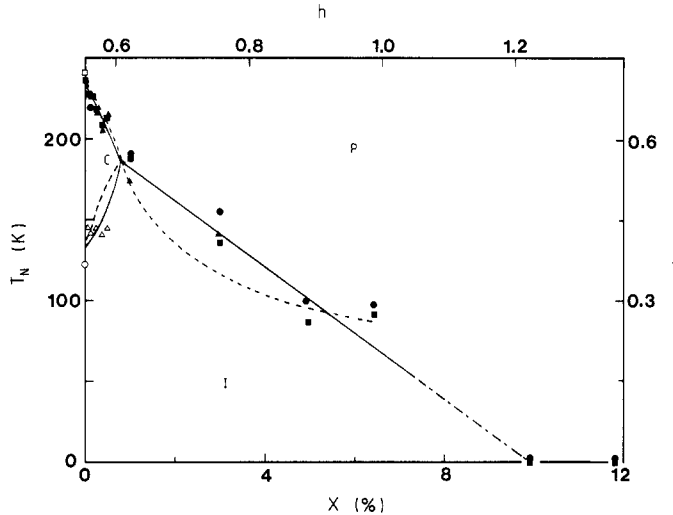
Figure 5. The magnetic phase diagram of $(Cr_{1-x}Mo_x)_{0.986}Si_{0.014}$ (full curves and line) for $0 < x \leq 12\%$. The I-P and C-P magnetic phase transition boundaries determined from the α-measurements are denoted by ▲ and the I-C phase transition is denoted by △. In the case of ρ and v_L measurements, the I-P and C-P magnetic phase boundaries are denoted by ● and ■, respectively. The points marked ○ for T_{IC} and □ for T_N of $Cr_{0.986}Si_{0.014}$ were taken from the work of Alberts and Lourens (1988). The broken lines represent the phase boundaries calculated from the two-band imperfect nesting model (Machida and Fujita 1984) displaying the reduced Néel temperature t ($= T/T_{N_0}$) as function of the misfit parameter h ($= H/\delta_0$). Note the two alloys $x = 0.10$ and 0.12 that remain paramagnetic at all T.

The transition temperatures, T_N and T_{IC}, of $(Cr_{1-x}Mo_x)_{0.986}Si_{0.014}$ are plotted as a function of x in figure 5. The average error in the absolute value of the transition temperatures amounts to ± 5 K. The consistency among the different independent sets of measurements is fairly good. The fact that I-C as well as CSDW-P transitions were observed in alloys with $0 < x \leq 0.005$ and only ISDW-P transitions for alloys with $0.01 \leq x \leq 0.05$, suggests the existence of a triple point where the ISDW, CSDW and paramagnetic states coexist somewhere between $x = 0.005$ and $x = 0.01$.

3. Discussion

The main difference between the magnetic phase diagrams of the Si series and Mo series of the Cr–Mo–Si system is that the latter displays a region of a CSDW state which was absent in the Si series. In the Si series the alloys remain ISDW at $T < T_N$ for all Si concentrations (Smit and Alberts 1989).

The Néel temperatures of the Mo series decrease by roughly 28 K / at.% Mo (for the first 1% added, they decrease by nearly 50 K). This should be compared to the case of binary Cr–Mo alloys where the addition of Mo decreases T_N linearly by 13 K / at.% Mo which is only about one half of the value observed for the Mo series. In the case of Mo in Cr this decrease is attributed to the combined effects of

d-band broadening (Cywinski and Hicks 1986) and impurity scattering (Behera and Viswanathan 1969). Behera and Viswanathan (1969) estimated the effects of impurity scattering in Cr–Mo as a decrease of 10 K / at.% Mo added. This leaves an additional decrease of 3 K / at.% Mo due to d-band broadening and possible changes in the density of states. Furthermore, Mo addition to pure Cr does not change the ISDW state of Cr to a commensurate one. Considering the much larger effect of Mo on T_N of the Mo series of Cr–Mo–Si alloys as well as the fact that the CSDW phase is completely suppressed when more than about 0.8% Mo is added (figure 5), we conclude that the observed effects cannot be explained by impurity scattering and d-band broadening effects alone, but that changes in the nesting parameter H must play a major role in the Mo series. The disappearance of the CSDW state in figure 5 can only be realised by a changing H on alloying with Mo.

We therefore proceed by fitting the theory of Machida and Fujita (1984) in which the phase transition lines are calculated in terms of H, to the experimentally observed phase diagram. They introduced a dimensionless parameter, $h = H/\delta_0$, where δ_0 is the energy parameter corresponding to the SDW energy gap at temperature T for $H = 0$, that is where k_e and k_h are equal, giving perfect nesting. A second parameter ρ, which is an indication of the size of the electron reservoir which originates from a third band, is also introduced. It is defined by $\rho = \rho_r/\rho_{e-h}$, where ρ_r is the reservoir density of states and ρ_{e-h} that of the electron–hole system. ρ plays an important role in determining the ISDW–CSDW phase line.

According to Machida and Fujita (1984) the magnetic phase boundary between the CSDW and paramagnetic phases is given by

$$\ln\left(\frac{1}{t_N}\right) + \mathrm{Re}\left[\psi\left(\frac{1}{2}\right) - \psi\left(\frac{1}{2} + \frac{i\nu h}{2\pi t_N}\right)\right] = 0 \qquad (2)$$

Here ψ is a digamma function, $\nu = 1.764$ and $t_N = T/T_{N_0}$ with T_{N_0} the Néel temperature for perfect nesting, $h = 0$.

At the triple point $h = 0.608$ and $t_N = 0.561$ (Machida and Fujita 1984). Taking this value of h as corresponding to an estimated triple point of concentration $x = 0.8\%$ (we could only determine it to lie somewhere between 0.5 and 1.0%) and temperature 185 K yields $T_{N_0} = 331$ K. This value gives $t = 0.711$ at $x = 0\%$ corresponding to $h = 0.554$ at this concentration. The broken CSDW–P line of figure 5 gives the best fit of equation (2) determined with the help of figure 2 of Machida and Fujita (1984) and the above values for h and t. Using their figure 2 and the correspondence between h and Mo concentration, x, determined above, we also calculated the position of the ISDW–P transition line as shown in figure 5.

The work of Machida and Fujita (1984) was also used to calculate the phase boundary line between the CSDW and ISDW phases. The C-I boundary is determined by

$$h = \tilde{h} - \frac{\pi}{4}\left(\frac{1}{1+\rho}\frac{\partial\Delta\Omega(t,\tilde{h})}{\partial\tilde{h}}\right)$$

where $\tilde{h} = \tilde{H}/\delta_0$ with $\tilde{H}$ a shifted misfit parameter, shifted due to a shift in the chemical potential when the SDW is formed. $\Delta\Omega(t,\tilde{h})$ is the change in the grand potential. From a table of values of $\tilde{h}$ and $\frac{1}{4}\pi\partial\Delta\Omega/\partial\tilde{h}$ for different t (Machida private communication) and using $\rho = 4.2$, we calculated the I-C transition line shown in

figure 5. This value of ρ was determined by applying the above equation at $x = 0\%$. At this concentration t is given by 0.403, corresponding to the mean experimental value of $T_{\mathrm{IC}} = 134$ K. These values of h and t mark the initial point on the theoretical I-C phase line and also determine the value of ρ.

The fit of the theory with acceptable values of h and ρ, to the phase diagram of figure 5 is fairly good except for the I-P transition line where the theoretical curve shows an upwards curvature while the experimental points decreases approximately linear with increasing concentration. This difference may possibly be attributed to the effects mentioned previously which are not included in Machida and Fujita's (1984) theory. These are impurity scattering effects, d-band broadening and effects due to changes in the density of states near the Fermi surface on alloying. At present it is not known how to include these effects in the theory of Machida and Fujita, but as explained previously, the first mentioned effect is expected to be the largest of the three effects. Impurity scattering will always lower T_{N} with the effect being larger the larger the Mo concentration. When this effect is included in the theory one would therefore expect the upwards curvature of the theoretical I-P transition line to diminish. This together with the fact that other h values are to be used in a theory that includes impurity scattering, would then probably give a better fit with the observed I-P transition line.

We conclude that changes in H play a major role in stabilising the different magnetic phases of the Mo series of ternary Cr–Mo–Si alloys. The fact that increasing Mo content corresponds to an increase in the misfit parameter h, points to a situation where Mo acts as an electron acceptor when added to the Mo series. This is in contrast to the binary Cr–Mo series, where Mo is accepted (Cywinski and Hicks 1986) to a first approximation not to change the e/a ratio. In the work of Cywinski and Hicks (1986) on Cr–Mo alloys it was found that the SDW Q-vector decreases slightly on addition of Mo. This may be taken as evidence that even in binary Cr–Mo alloys, Mo acts slightly as an electron acceptor.

4. Conclusion

The magnetic phase diagram of a Mo series of ternary Cr–Mo–Si alloys displays both CSDW and ISDW phases with a triple point at about 0.8% Mo. This is in contrast to the Si series in which the CSDW phase was absent. The magnetic phase diagram of the Mo series is fairly well explained by assuming changes in the nesting parameter on alloying to be the dominant effect. Effects of d-band broadening, attributed to a gradual delocalization of d-wave functions as the 4d Mo electrons replace the 3d electrons of Cr, and impurity scattering effects as well as changes of density of states on alloying, have also to be considered in the final analysis. These effects combined, however, may play a smaller role as the effects of alloying on the nesting parameter. Mo appears to act as an electron acceptor in the Mo series.

Acknowledgments

References

Alberts H L private communication
Alberts H L and Lourens J A J 1983 *J. Phys. F: Met. Phys.* **13** 873
—— 1984 *Phys. Rev.* B **29** 5279
—— 1988 *J. Phys. F: Met. Phys.* **18** 123
Behera S N and Viswanathan K S 1969 *Can. J. Phys.* **47** 477
Cywinski R and Hicks T J 1986 *J. Magn. Magn. Mater.* **54–57** 999
Dadărlat D, Guirgiu A and Pop I 1980 *Solid State Commun.* **34** 109
Endoh Y, Mizuki J and Ishikawa Y 1982 *J. Phys. Soc. Japan* **51** 2826.
Fujita M and Machida K 1987 *J. Magn. Magn. Mater.* **70** 442
Koehler W C, Moon R M, Trego A L and Mackintosh A R 1966 *Phys. Rev.* **151** 405
Lomer W M 1964 *Proc. Phys. Soc.* **84** 327
Machida K private communication
Machida K and Fujita M 1984 *Phys. Rev.* B **30** 5284
Roberts R B, White G K and Fawcett E 1983 *Physica* B **119** 63
Smit P and Alberts H L 1986 *J. Phys. F: Met. Phys.* **16** L191
—— 1987 *J. Phys. Chem. Solids* **48** 887
—— 1989 *J. Phys. : Condens. Matter.* **1** 5731
Van Rijn H J, Alberts H L and Lourens J A J 1987 *J. Phys. Chem. Solids* **48** 283
Venter A M, Alberts H L and Lourens J A J 1986 *J. Magn. Magn. Mater.* **62** 269